

brian.colle@stonybrook.edu

Brian A. Colle¹, Aaron R. Naeger², and Andrew Molthan³

¹School of Marine and Atmospheric Science, Stony Brook University, Stony Brook, NY, ²University of Alabama in Huntsville, Earth System Science Center/NASA SPoRT, Huntsville, AL

³NASA Marshall Space Flight Center/Earth Science Office, Huntsville, AL

Motivation and Goals

- Over the GCPEX study domain (Fig. 1) on 18 February 2012 a warm frontal precipitation band rapidly evolved from genesis, maturity, and decay from 0730 UTC to 1334 UTC 18 February 2012 (Fig. 2).
- Narrow and intense bands have been well documented for cold fronts, but not for warm fronts. The conceptual model of a warm frontal band is fairly broad (~50 km wide), with a strong connection to generating cells aloft.

Questions:

- What processes led to the rapid intensification and subsequent weakening of the warm frontal precipitation band?
- What is the role of latent heating and cooling on the band evolution?
- How did the ice and water amounts change within the band as it evolved?
- How well can a mesoscale model predict this warm frontal band evolution?

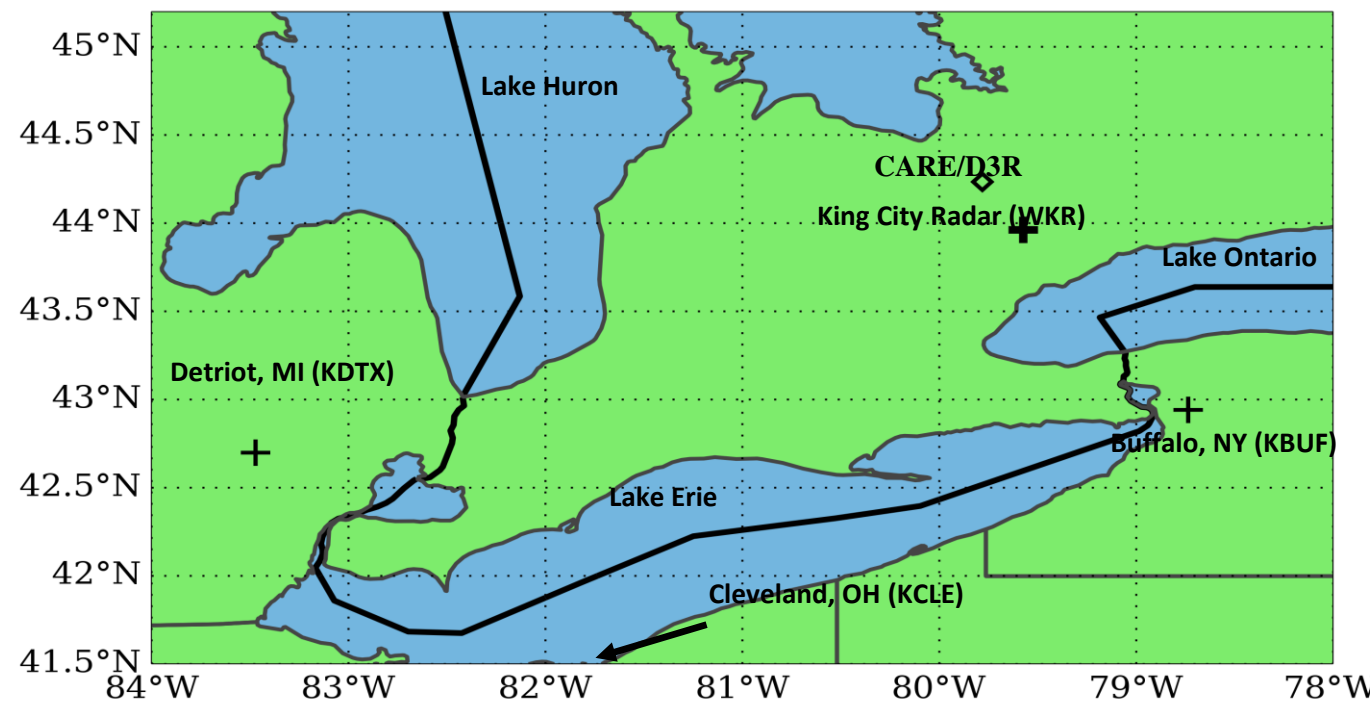


Figure 1. Map of the GCPEX field campaign region depicting the locations of the CARE ground instrumentation site along with the locations of the King City and dual-frequency, dual-polarized Doppler radar (D3R). Note the D3R was stationed at the CARE site. The locations of the WSR-88D radar sites at Buffalo, NY (KBUF), Detroit, MI (KDTX), and Cleveland, OH (KCLE), which are used in this study, are also shown on map. The KCLE radar site is located approximately 10 miles south of the arrow endpoint.

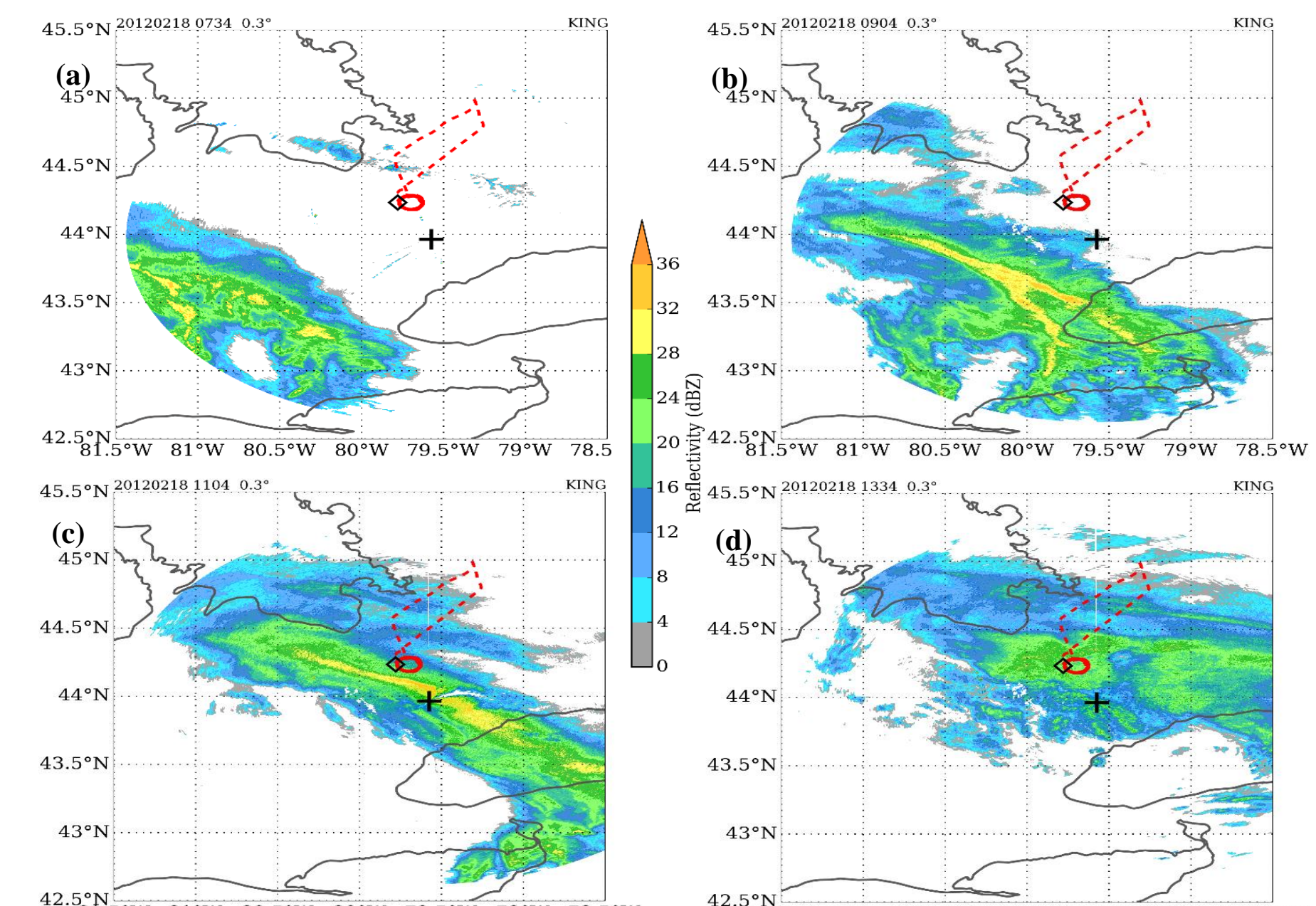


Figure 2. Reflectivity (shaded in dBZ) from the 0.3 degree elevation scan from the King City radar (black cross) at (a) 0734 UTC, (b) 0904 UTC, (c) 1104 UTC, and (d) 1334 UTC 18 February 2012.

Model Setup and Configuration

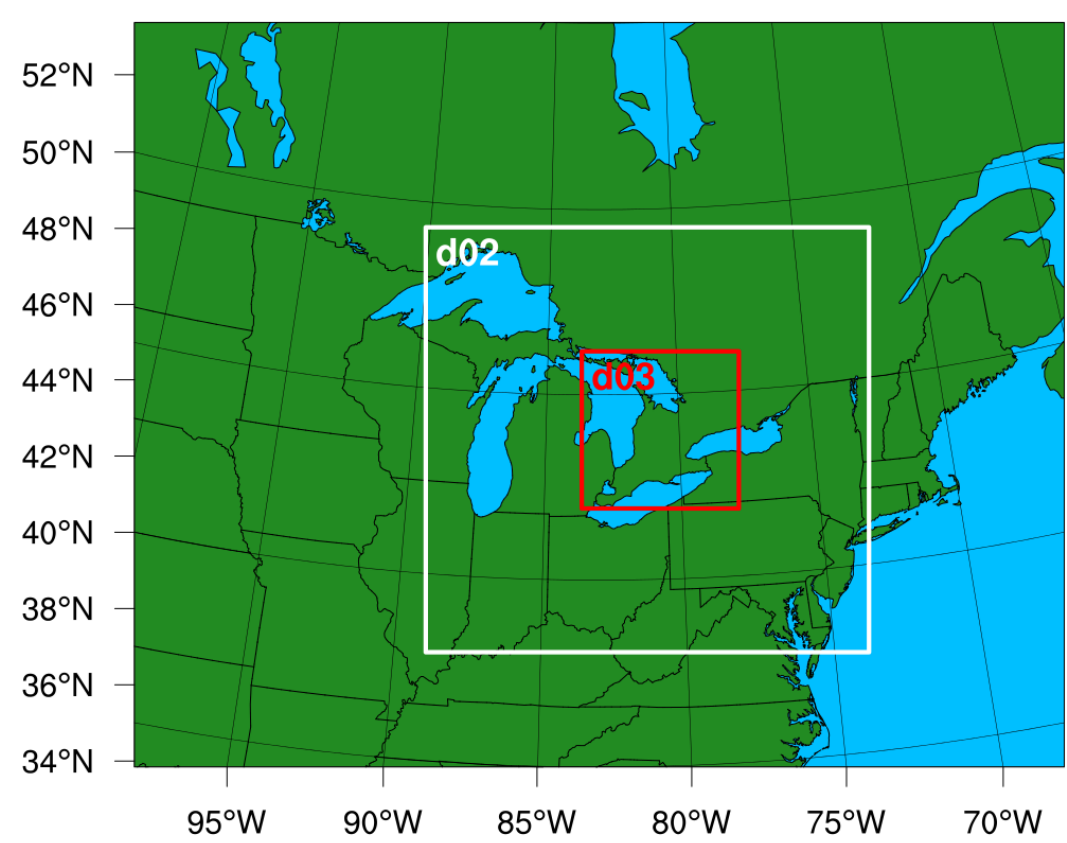


Figure 3. WRF model grid configuration

NU-WRF configuration options			
Boundary Condition Data	RUC		
Vertical Resolution	50 Levels		
PBL Physics	Mellor-Yamada-Janjic scheme		
Cloud microphysics	P3 (Morrison and Milbrandt 2015)		
Shortwave Radiation	RRTMG		
Longwave Radiation	RRTMG		
Domains	Domain 1	Domain 2	Domain 3
Horizontal Resolution	9 km	3 km	1 km
Grid Points	301x241	430x412	457x457
Cumulus scheme	Grell-Devenyi	Turned off	Turned off

Table 1. NU-WRF configuration options

- The Advanced Research WRF (Weather Research and Forecasting; Skamarock et al. 2008) model version 3.5.1 was used for a 30-h run with a triple-nested grid configuration at 9-, 3-, and 1-km horizontal grid spacing (Fig. 3).
- Forecasts were initialized at 1800 UTC 17 February 2012 with initial and lateral boundary conditions from 6-hourly 13-km isobaric RUC analyses.
- All ice-phase particles in the P3 scheme are represented by four mixing ratio variables (total mass, rime mass, rime volume, and number) that freely evolve in time and space.

Warm Frontal Band Development

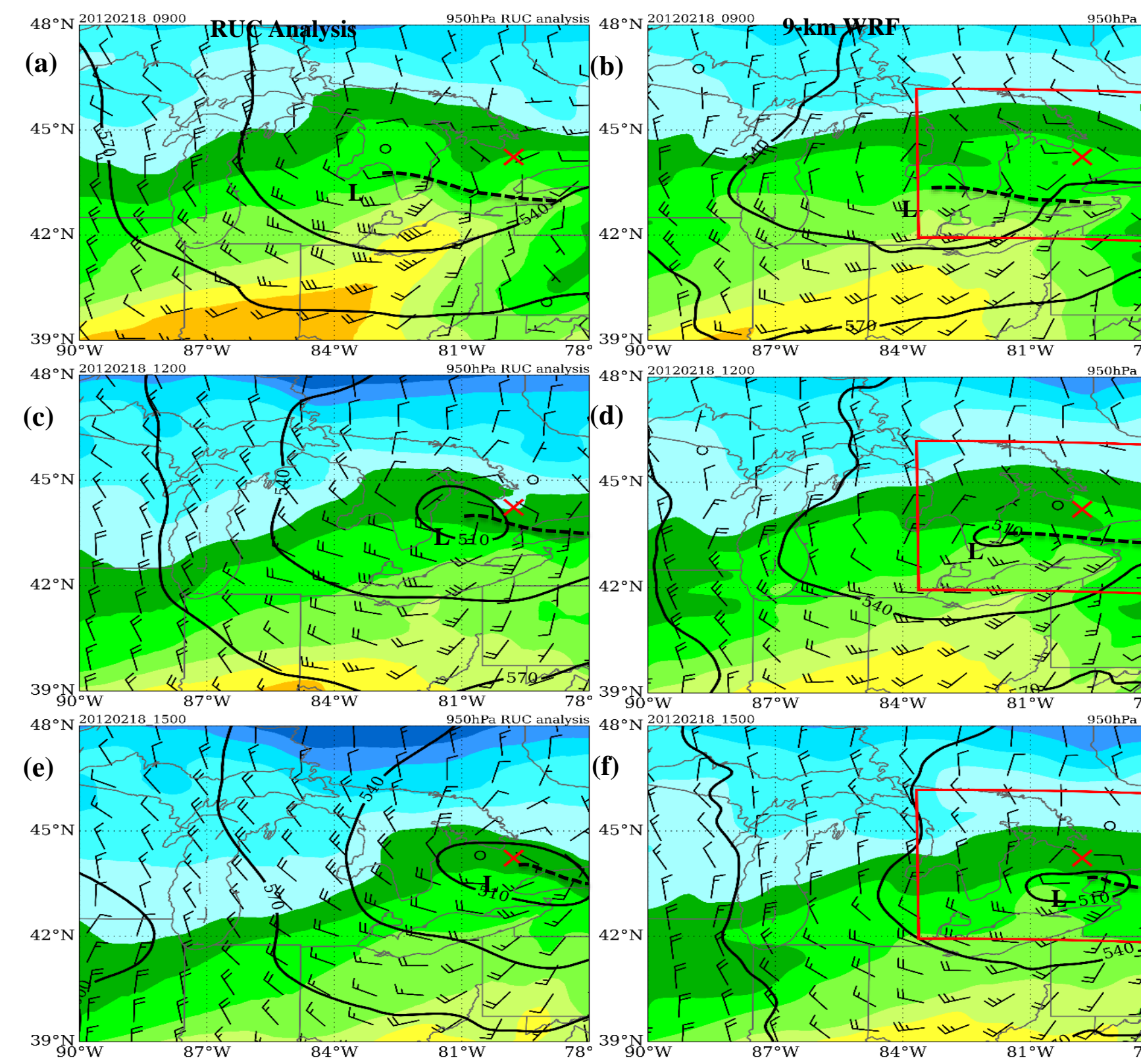


Figure 4. RUC analysis (left) and 9-km WRF (right) 950 hPa geopotential heights (solid black, contoured every 30 m), temperature (shaded), and winds (1 full barb = 10 kt) at (a),(b) 0900, (c),(d) 1200, and (e),(f) 1500 UTC 18 February 2012. GCPEX field campaign region is indicated by the red X and the location of the 1 km inner nested grid is shown by the red box. Low pressure circulation center is indicated by L and the associated warm front is shown by the dashed black line.

- There was a relatively weak surface cyclone (~1012 hPa) located near the study area of southwest Ontario (not shown), with a relatively weak surface warm front stretching to the east of the cyclone (Fig. 4).

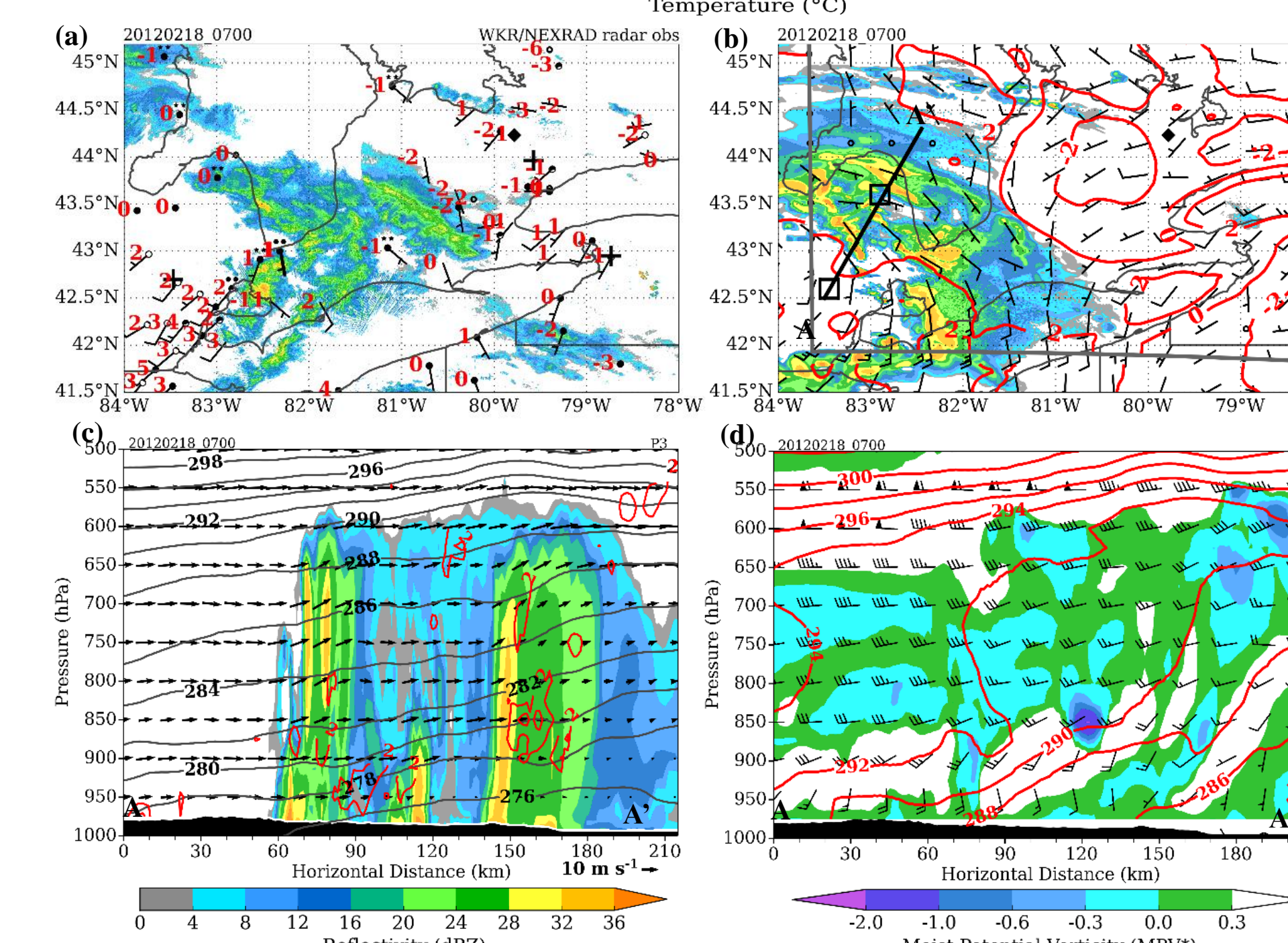


Figure 5. (a) Horizontally polarized radar reflectivity (shaded in dBZ) from the 0.3° elevation scan of the King City radar and 0.5° elevation scans of the KBUF (Buffalo, NY), KCLE (Cleveland, OH), and KDTX (Detroit, MI) WSR-88Ds (black crosses) at approximately 0700 UTC 18 February 2012. Automated surface observation station measurements of 2-m temperature (°C) and 10-m wind speed (1 full barb = 10 kts) at 0700 UTC are also shown. (b) WRF simulated reflectivity (shaded) at 0700 UTC from the lowest model vertical level based along with predicted 2-m temperature (red, contoured every 2°C) and 10-m wind speed. GCPEX ground instrumentation CARE site is indicated by solid diamond. The output from the 1-km WRF domain is displayed within the domain boundaries (thick gray) while the 3-km WRF output is displayed everywhere outside these boundaries. (c) Cross-section (AA') across precipitation area in (b) showing simulated reflectivity (shaded), potential temperature (gray, contoured every 2 K), Pettersen frontogenesis (red, contoured every 4°C 100 km⁻¹ h⁻¹ starting at 2°C (100 km⁻¹ h⁻¹), and three-dimensional wind circulation vectors (vertical velocity multiplied by factor of 20 relative to horizontal velocity). (d) Same cross-section as in (c) but showing MPV* (shaded), q_e* (red, contoured every 2 K), and horizontal winds.

- Band genesis began in an area of precipitation with embedded convection to the north of the warm front in a region of weak frontogenetical forcing at low-levels and a weakly positive to slightly negative moist potential vorticity (MPV*) from 900-650 hPa (Figs. 5-6).

Figure 6. Same as Fig. 5 except for 1130 UTC 18 February 2012.

Microphysical Evolution

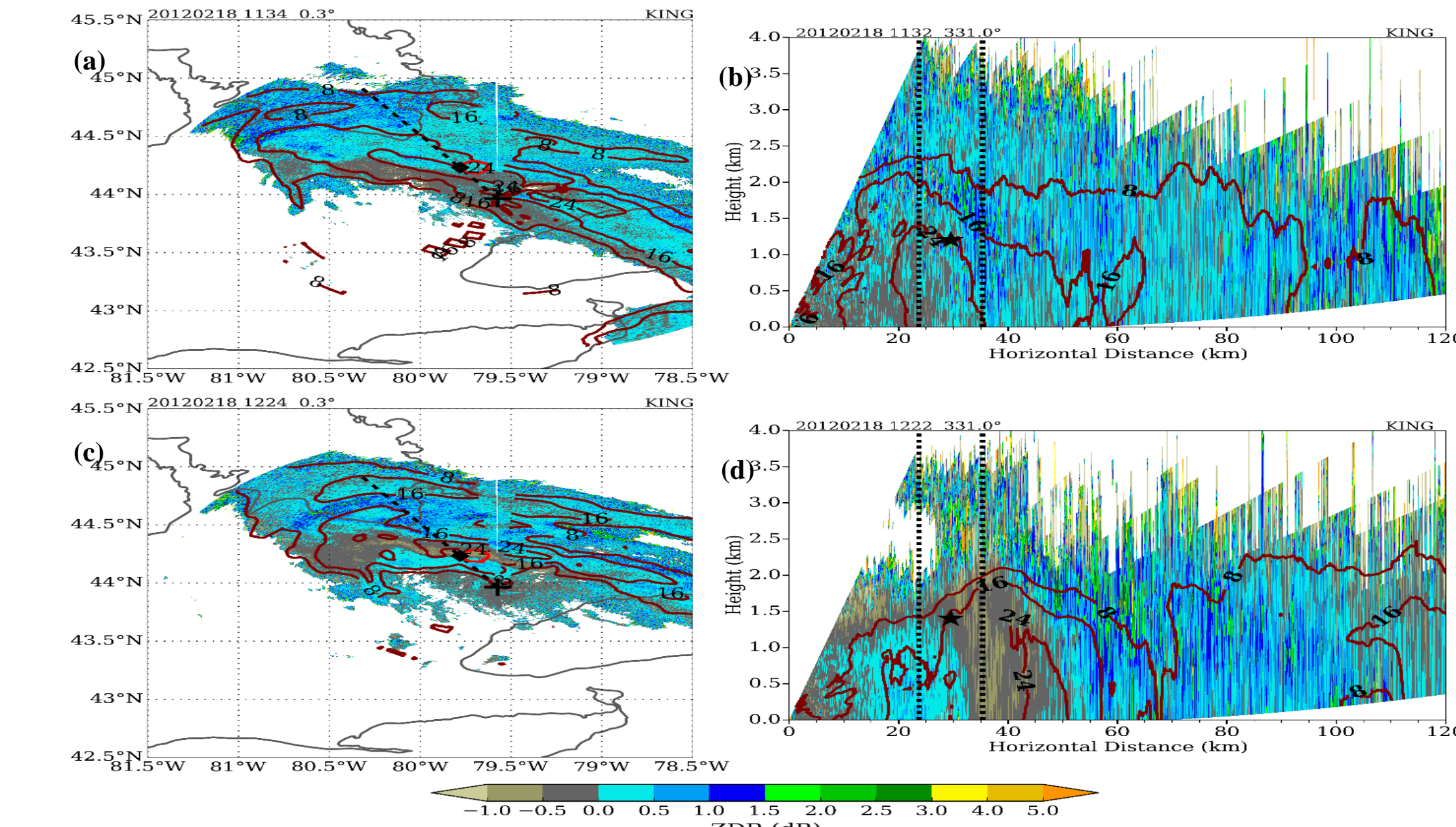


Figure 7. King City radar observations of ZDR (shaded in dB) and dBZ (maroon, contoured every 8 dBZ starting at 8 dBZ) from (a) PPI and (b) RHI scans valid at 1124 and 1122 UTC 18 February, respectively. (c,d) Same as in (a), (b) except observed at 1234 and 1232 UTC, respectively. Aircraft spiral flight pattern (red) is denoted in (a) and (c) and location where the flight intersected the RHI scan (vertical dashed red lines) is denoted in (b) and (d). The red star in (b) and (d) denotes location of aircraft 2DC probe samples in Fig. 16b and 17b.

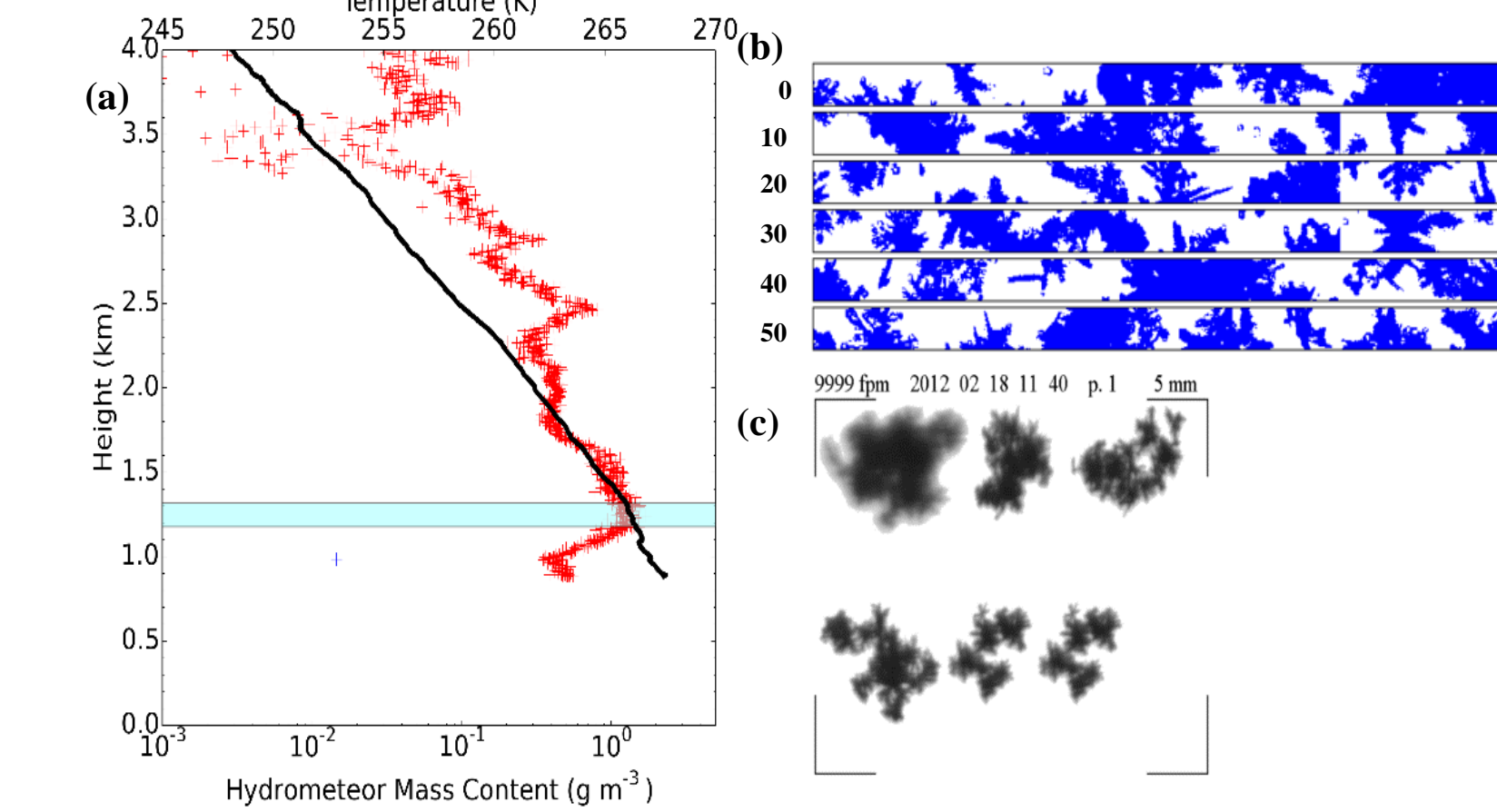


Figure 8. (a) Liquid water (blue cross; negligible amounts at this time) and ice water content (red cross) profiles along with temperature (black) from aircraft descent through the observed band between 1122 and 1143 UTC on 18 Feb 2012. (b) Aircraft ice habits from the 2DC near 1.2 km in height (blue shaded region in (a)) at 1140 UTC within the band and (c) those collected at the surface by the CARE site PVI (camera 1 with horizontal optical axis) at the same time. 2DC samples particles in size range from 30-960 μm with 30 μm resolution, and samples acquired every 10 seconds within one minute flight time at 1140 UTC are shown.

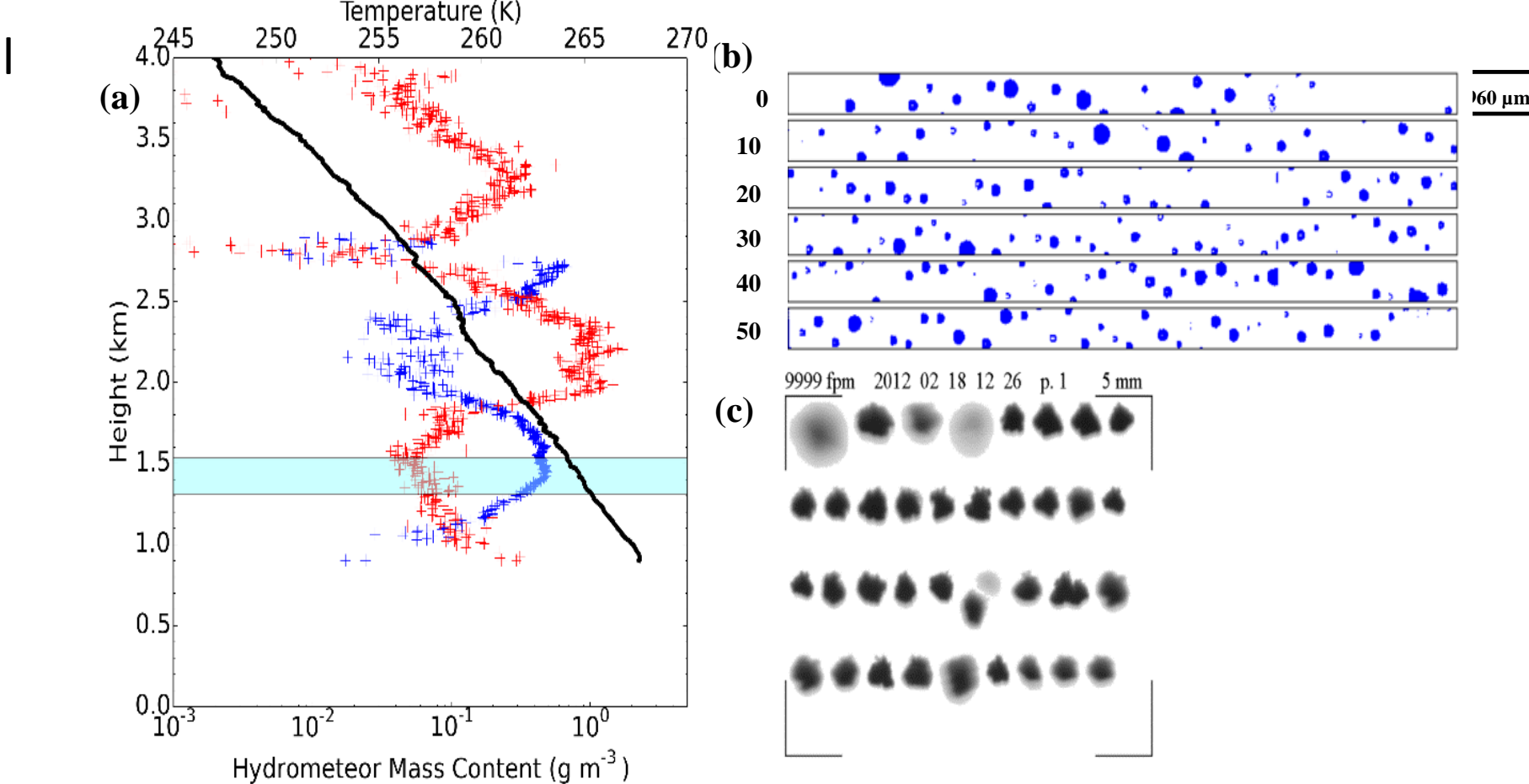


Figure 9. Same as in Fig. 8 except measurements from aircraft ascent between 1223 and 1242 UTC are shown, and 2DC particle samples were from about 1.4 km in height at 1225 UTC. CARE site PVI sample was one minute later at 1226 UTC.

- At 1124 UTC, the ZDRs are near zero or slightly positive within the band, and the correlation coefficients are relatively high (> 0.99 (not shown), suggesting horizontally falling snow crystals and aggregates. The ZDRs are more negative to the south of the band and at ~1225 UTC, indicative of graupel (Fig. 7).

- Aggregates of unrimed snow occurred within the band during early maturity, while more supercooled water and graupel occurred as the upward motion increased due to the frontogenetical circulation. (Figs 8-9).

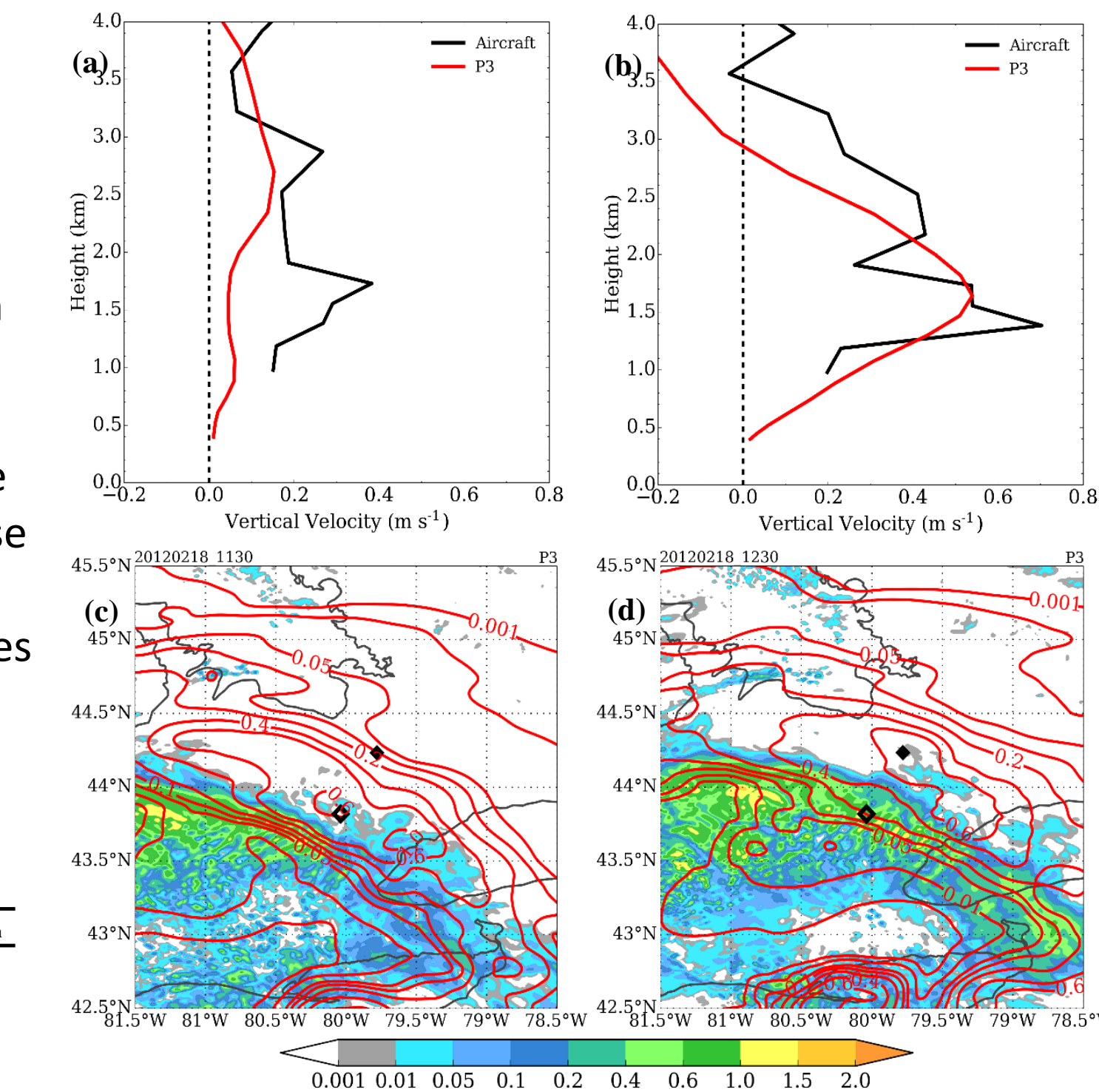


Figure 10. (a) Vertical motion (30-s average) from aircraft descent (black) from Fig. 16a and 1 km WRF model output (red) at 1130 UTC. (b) Vertical motion from aircraft ascent (black) from Fig. 17a and 1 km WRF model output (red) at 1230 UTC. Cloud liquid water (shaded) and ice water path (red, same contour intervals as cloud liquid water) from 1 km WRF model output at (c) 1130 UTC and (d) 1230 UTC.

Summary

The band developed with low-level deformation and frontogenesis along the sloping warm frontal zone, and the vertical motions became large enough to produce graupel on the south side of the band. Embedded convective cells developed earlier in our GCPEX event, but the frontogenesis was weak then and banding was limited. As the deformation increased the stability also increased near the banding location (MPV* ~ 0), which favored the development of single band. Through sensitivity studies (not shown) we found that latent heating helps increase the frontal circulations and resulting band development. Latent cooling also helps increase the frontogenesis given the evaporative and sublimation cooling within the frontal precipitation.

* This work was supported by grant NASA NNX13AF88G.